JOURNAL OF SPACECRAFT AND ROCKETS
Vol. 30, No. 6, November–December 1993

Winged Booster Performance with Combined Rocket and Airbreathing Propulsion

Roger A. Lepsch, Jr.* and J. Christopher Naftel*
NASA Langley Research Center, Hampton, Virginia 23665

A conceptual level analysis was performed on a horizontal-takeoff, two-stage-to-orbit system consisting of a rocket and turboramjet powered hypersonic booster and a rocket-powered orbiter. The analysis includes estimates of vehicle aerodynamics, performance, and weights. Rocket and airbreathing systems on the booster are operated in parallel and at full thrust for ascent to a Mach 6 staging point, whereas cruise back is accomplished using airbreathing propulsion alone. Rocket engines on the orbiter are ignited at staging to propel the orbiter. Booster weights were determined for various combinations of rocket and airbreathing propulsion. The combinations that resulted in the lowest vehicle gross and empty weights were determined. Results show that the lowest gross weight occurs when only airbreathing engines are used. The empty weight of the all airbreathing booster, however, is quite high. Significant reductions in booster empty weight is accomplished with the addition of rocket engines. Also, the use of rockets on the booster greatly decreases the time to staging and the cruise-back distance.

Nomenclature

g	=gravitational acceleration, 32.2 ft/sec^2
I_s	=engine specific impulse (thrust/flow rate), s
M	=Mach number
O/F	=oxidizer-to-fuel ratio
P_c	=chamber pressure, psia
T/W	=thrust-to-weight ratio
T/A_e	=thrust-to-exit-area ratio
V_P	=total propellant volume, ft^3
W_P	=total propellant weight, lb
ρ_{bulk}	=propellant bulk density, lb/ft^3

Introduction

CONCEPTS currently being considered as candidates for the nation's next manned space transportation system include those powered by airbreathing propulsion for ascent. Airbreather engines have high specific impulse compared with rocket engines since the oxidizer is obtained from the atmosphere and not carried onboard the vehicle as propellant. As a result, operational capabilities, such as cruise, self-ferry, and landing go-around are enhanced. These capabilities are difficult, or impossible, to achieve with all-rocket-powered vehicles. However, airbreathing engines of the size or quantity necessary to provide acceleration along significant portions of an ascent flight path are difficult to integrate into the vehicle. Airbreathing engines typically have low thrust-to-weight ratios, and much of the gain obtained by low propellant consumption is lost due to high propulsion-system weights. Adding rockets, which provide high thrust for low weight, reduces the number of airbreathing engines, therefore simplifying engine-airframe integration and reducing propulsion-system weight. Rockets have low specific impulse values however, and their use increases propellant consumption.

Numerous studies have been made of both two-stage and single-stage launch vehicle concepts that utilized a combination of rocket and airbreathing propulsion in the same stage for ascent acceleration. The rocket and airbreathing elements were either contained in separate engines or combined into a single engine, generally referred to as a rocket-based combined-cycle engine (RBCC). In the mid-1960s, Marquardt studied many RBCC options for use in the first-stage booster of a two-stage-to-orbit system.[1] The works of Bendot et al.,[2] Martin,[3,4] Kramer and Bühler,[5,6] Schoettle,[7] and Foster et al.[8] investigated the application of combined airbreathing/rocket propulsion, both with separate and RBCC engines, to single-stage-to-orbit vehicles. An example of a single-stage-to-orbit vehicle concept utilizing separate rocket and airbreathing engines is the Star-Raker, studied by Rockwell in the late 1970s.[9] Recent examples of combined airbreathing/rocket propelled vehicle concepts include the single-stage HOTOL[10] of the U.K.; the two-stage BETA,[11] studied for the U.S. Air Force; and the X-30 NASP.[12] Few of the concepts studied operate airbreathing and rocket propulsion in a parallel or mixed mode, and if so, only briefly. The BETA vehicle is unique in that the rocket systems on the booster and orbiter operate in parallel with the airbreathing systems on the booster during the ascent to staging.

Despite the number of combined airbreathing/rocket vehicle concepts studied, little effort was expended on optimizing vehicle performance and weights by separately varying both airbreathing- and rocket-propulsion elements. Nor has there been a determination if extensive mixed-mode operations are beneficial. Presented in this paper are the results of a conceptual level analysis of a near-term, horizontal-takeoff, two-stage-to-orbit system consisting of a combined airbreathing/rocket-propelled booster and a rocket-propelled orbiter. To gain a basic understanding of the effects of combined airbreathing and rocket propulsion on vehicle characteristics, the propulsion systems of the booster were maintained separate and the amount of rocket and airbreathing propulsion were varied over a wide range. Parallel operation of the booster-propulsion systems was assumed from takeoff to a Mach 6 staging point. Variations in the weights, propellant characteristics, time to staging, and downrange distance of the booster as a function of both airbreathing and rocket thrust are summarized.

Vehicle Description

The launch-vehicle configuration chosen for this study is shown in Fig. 1. It is similar to the two-stage-to-orbit German Sänger concept,[13] which in turn is similar to several designs investigated in the United States in the mid-1960s.[1,14] The system consists of a large, airbreathing hypersonic booster with a rocket-powered orbiter partially recessed in the upper fuselage. The design is appropriate for staging velocities in the Mach 6–7 range. The main difference between this design and similar designs previously

Presented as Paper 92-3500 at the AIAA/SAE/ASME 28th Joint Propulsion Conference, Nashville, TN, July 6–8, 1992; received Sept. 17, 1992; revision received Dec. 16, 1992; accepted for publication Dec. 16, 1992.

*Aerospace Engineer, Space Systems Division. Member AIAA.

studied is the incorporation of a rocket system on the booster in addition to an airbreathing system. The technology level assumed for the vehicle is near-term, with an initial operational capability date of 2002, and is reflected in the propulsion performance, material temperature limits, and weight estimates.

The airbreathing-propulsion system utilized for the booster is a hydrogen-fueled turboramjet. A schematic of the engine installation is shown in Fig. 2. The turboramjet combines turbojet and ramjet propulsion cycles in the same engine. The engine operates as an afterburning turbojet from low speed up to Mach 3, then transitions to ramjet operation for higher speeds. The turbojet and ramjet sections of the engine are arranged in tandem, where airflow bypasses the turbojet section during high-speed flight. Maximum speed of operation in the ramjet mode is limited in this study to Mach 6 due to engine temperature limitations. In general, the subsonic combustion ramjet is capable of operation up to Mach 8, but beyond Mach 6 performance degrades rapidly due to the dissociation of combustion products. These engines are located in a side-by-side arrangement on the bottom of the fuselage. Estimated performance and weights for an installed engine (accounting for inlet and nozzle) were based on data obtained from Ref. 15. Performance specifications are listed in Table 1 for the size engine assumed for this study.

The rocket-propulsion system utilized for the booster is the linear aerospike rocket engine fueled by liquid hydrogen (LH_2) and liquid oxygen (LOX).[16] The rockets are installed in the aft body of the vehicle in the area between the vertical tails (Fig. 3). The aft body is used as an isentropic expansion surface for the rockets. The anticipated advantages of using the linear aerospike rocket over those of a conventional bell-nozzle rocket are lower weight and lower base drag resulting from fuselage/engine integration. Table 2 lists engine specifications.

The rocket-propulsion system assumed for the orbiter consists of conventional LOX-LH_2 bell-nozzle rockets. Performance, in terms of specific impulse, is equivalent to a high expansion ratio derivative of the Space Shuttle main engine. This engine has a vacuum I_s of 462.5 s with an expansion ratio of 150:1 and a LOX/LH_2 mixture ratio of 6.

Mission Description and Trajectory

The mission for the vehicle is to service a manned space station located in a 220-n.mi. orbit with an inclination of 28.5 deg. The required on-orbit stay time for the orbiter is 1 day with a crew of five. The orbiter is required to deliver and return a nominal payload of 7300 lb. Launch and recovery is to be performed at the Kennedy Space Center.

The typical flight profile is presented in Fig. 4 and consists of the following. The vehicle performs a horizontal takeoff, climbs and accelerates at constant dynamic pressure to hypersonic speed, then performs a pull-up maneuver to reduce dynamic pressure and increase flight-path angle for release of the orbiter. The orbiter separates after engine ignition and continues on to orbit insertion along a typical, high-flight-path-angle rocket trajectory. After staging, the booster performs an unpowered decelerating turn maneuver, then cruises back subsonically on airbreathing power to the launch site. Upon completion of the mission, the orbiter reenters the atmosphere and returns for an unpowered landing.

To remain within near-term turboramjet and airframe material limitations, the dynamic pressure during the booster ascent is limited to 1000 lb/ft^2 and the maximum velocity prior to staging is limited to Mach 6. The dynamic pressure at staging is constrained to 300 lb/ft^2, to reduce aerodynamic loads during the separation maneuver. Maximum axial acceleration during ascent is limited to 3 g for both the orbiter and the booster. The normal force limits on the orbiter and booster are 2.5 g and 2 g, respectively.

For vehicle ascent to the staging point, two types of flight paths were devised to accommodate the large thrust range possible when using both rocket and airbreathing propulsion; a low T/W path, and a high T/W path. The flight paths are illustrated in Fig. 5. The low T/W path is tailored to contain a shallow dive in the transonic region to help the vehicle overcome the higher drag encountered there. A maximum velocity of Mach 6 is reached along the constant dynamic pressure path, but because of the low T/W, speed decreases after pull-up, and staging occurs at a slightly lower velocity. The high T/W path is followed when the vehicle has a large amount of excess thrust. The dive at transonic speed is eliminated, but an earlier pull-up is required to prevent acceleration beyond the Mach 6 maximum velocity. The engines are not throttled during ascent unless axial acceleration limit is reached. For

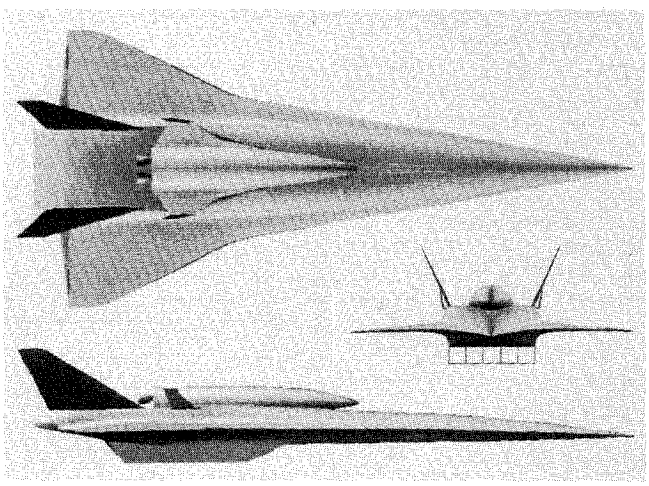

Fig. 1 Vehicle configuration.

Table 1 Turboramjet engine specifications

Installed sea level thrust at $M=0.454$, lb	78,600
Installed sea level I_s at $M=0.454$, s	4,766
Compressed exit temperature limit, °F	1160
Stator outlet temperature, °F	2780
Overall pressure ratio	12.0
Inlet capture area, ft^2	16.7
Engine diameter, ft	6.5
Turbojet/ramjet transition Mach	3.0
Weight (including inlet), lb	24,100
Fuel	LH_2

Table 2 Linear aerospike rocket engine specifications

Propellants	LOX-LH_2
Cycle	Staged combustion
P_c, psia	2500
Expansion ratio	80
O/F	7
Sea level I_s, s	382
Vacuum I_s, s	453
Sea level T/W	67
Sea level T/W (w/o nozzle)	96.5
Sea level T/A_e, lb/ft^2	11,390

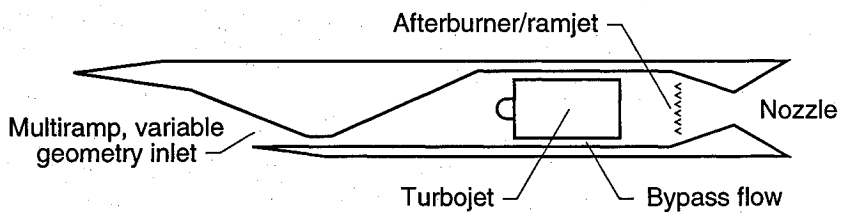

Fig. 2 Turboramjet engine.

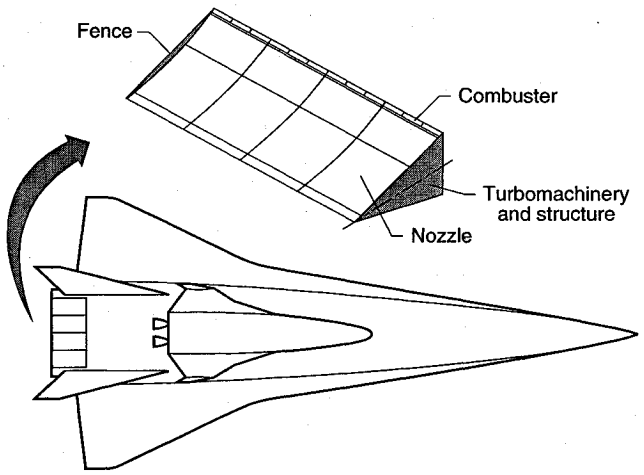

Fig. 3 Linear aerospike rocket installation.

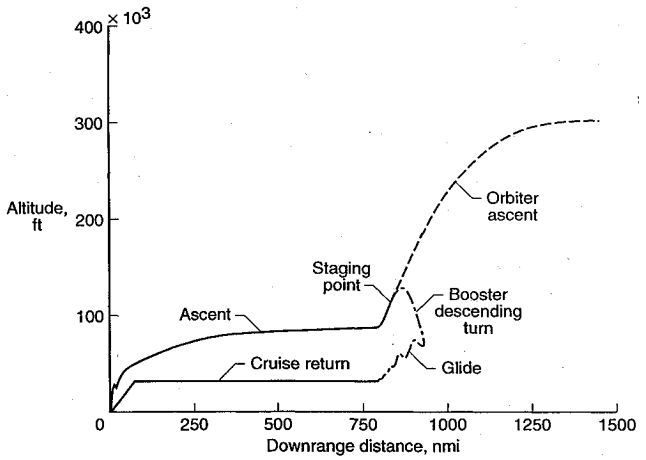

Fig. 4 Typical vehicle flight profile.

this study, vehicle ascent and booster cruise-return trajectories were simulated. Orbiter entry trajectory simulations were not performed.

Analysis

Method

The general procedure for determining the overall physical characteristics of a two-stage series-burn vehicle is to size the upper stage for a fixed payload and use this sized upper stage as the required payload to size the lower stage. Therefore, the physical characteristics of the orbiter were determined first based on the required orbital payload and the staging conditions. To simplify the analysis, small differences in the staging condition due to flight-path variations were neglected and a fixed staging condition was assumed. This allowed the analysis of the orbiter to be performed independent of the booster.

To determine the size and weight of the orbiter an analysis consisting of aerodynamics, performance, and component weights estimation was performed. The lift and drag coefficients of the orbiter shape were determined for a range of flight conditions and angle of attack. These coefficients were used as input to a trajectory simulator. Variations in the aerodynamic coefficients with vehicle scale were considered negligible, therefore the coefficients were assumed constant. An optimized trajectory simulation from the staging point to orbit insertion was performed in order to determine the required propellant fraction. For a constant initial *T/W*, this propellant fraction was assumed to be independent of the weight and size of the orbiter. This propellant fraction was then used with estimates of structure and subsystem weights to determine the size of the orbiter necessary to deliver the required payload. Sizing was performed by scaling orbiter geometry equally in all dimensions with the propellant-to-body-volume fraction assumed constant. To be conservative, the staging condition of the orbiter was selected to correspond to that of the low *T/W* type booster trajectory, which has a lower staging velocity. This results in the orbiter being slightly larger than necessary for the high *T/W* booster trajectories. The initial conditions for the orbiter were an altitude of 111,000 ft, a velocity of Mach 5.5, and a flight-path angle of 6 deg.

The size of the orbiter was used to determine the size of the booster based on the integrated shape of the configuration. This was done to eliminate the complicated task of reintegrating the orbiter and booster geometries as well as to maintain the same general aerodynamic characteristics of the mated configuration. Since the size of the orbiter was fixed as a result of fixed payload weight and staging conditions, the size of the booster was also fixed. However, propellant volume was allowed to vary within the fixed fuselage of the booster up to a determined maximum allowable value.

As with the orbiter, the weight of the booster was determined by an analysis consisting of aerodynamics, performance, and component weights estimation. The lift and drag characteristics of the mated configuration were predicted for several different wing sizes and tabulated as input for the trajectory simulations. This allowed the wing size to be adjusted according to gross weight in order to maintain a consistent takeoff speed. Based on the wing size derived from a fixed 75 lb/ft^2 takeoff wing loading, the aerodynamic characteristics for a specific gross weight were determined by interpolation. A trim analysis of the vehicle was not performed and the aerodynamic characteristics determined do not account for changes in the number of airbreathing engines. However, the characteristics were considered suitable for the overall level of analysis performed. To determine the weight of the booster required to deliver the fully loaded orbiter to the staging point for a specific rocket and airbreathing-propulsion system combination, trajectory simulations were performed for a range of vehicle gross weights. For each specific gross weight, the propellant fractions obtained from the trajectory simulation were used along with estimates of structure, subsystem, and cruise-back pro-

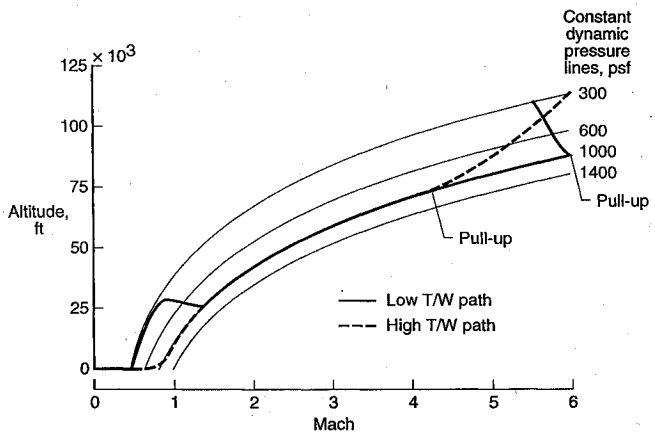

Fig. 5 Ascent flight path to staging.

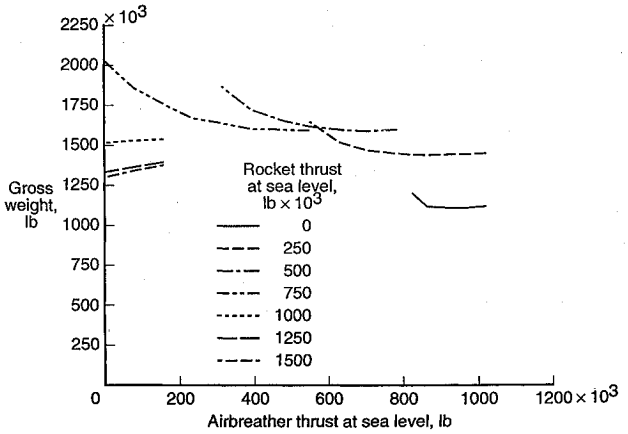

Fig. 6 Gross weight sensitivity to airbreather/rocket-thrust mix.

pellant weights to calculate the lift capacity of the booster. From a curve fit of this data, it was estimated at what gross weight, if any, the lift capacity matched the orbiter gross weight. A trajectory simulation was then performed with the gross weight obtained to verify the result.

Tools

Configuration aerodynamics were predicted using the aerodynamic preliminary analysis system (APAS).[17] The APAS is capable of analyzing three-dimensional configurations having multiple surfaces of arbitrary planform and bodies of noncircular contour. Analysis methods are based on potential theory at subsonic speeds and impact-type finite element solutions at hypersonic speeds.

Trajectories were simulated using the program to optimize simulated trajectories (POST).[18] The POST is a generalized, event-oriented trajectory program that can be used to analyze ascent, on-orbit, and entry trajectories. Any calculated variable in POST can be optimized although subject to a combination of both equality and inequality constraints.

The weights analysis was performed using the configuration sizing (CONSIZ) program. The CONSIZ program is capable of determining individual stage mass properties for a variety of launch-vehicle types. Options are available to determine payload weight capability given a fixed vehicle size or determine the size of the vehicle given a fixed payload weight. Sizing is performed by scaling the geometry of a point design vehicle equally in all dimensions, assuming a constant propellant volume packaging efficiency, until propellant fraction requirements obtained from a trajectory simulation are satisfied. Weight estimating relationships (WERs) corresponding to the vehicle components are input to the program and can be easily modified to incorporate updates when necessary. Statistically developed, historically based WERs were used for this analysis and were either obtained from sources on

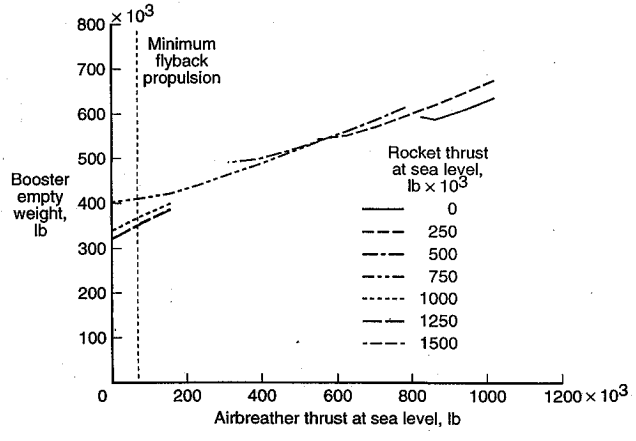

Fig. 7 Empty weight sensitivity to airbreather/rocket-thrust mix.

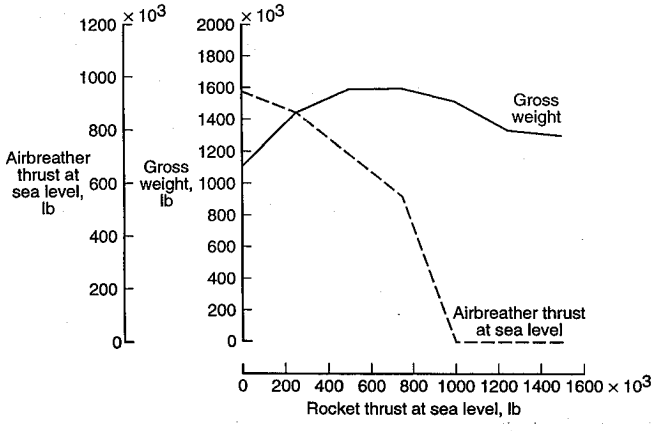

Fig. 8 Minimum gross weight and corresponding airbreather thrust as a function of rocket thrust.

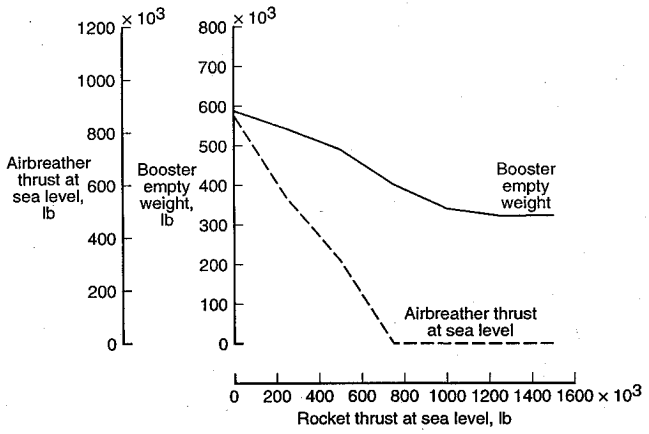

Fig. 9 Minimum empty weight and corresponding airbreather thrust as a function of rocket thrust.

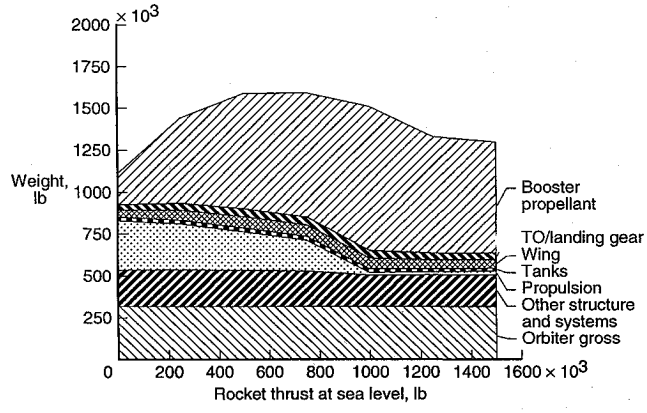

Fig. 10 Vehicle weight composition for minimum gross weight.

weight estimation methods[19–21] or were developed in-house using available weights data on existing aircraft and spacecraft. Space Shuttle weight reports[22,23] were used as a primary source of information for many vehicle systems. Appropriate adjustments to the WERs were made to update to a near-term technology level.

Vehicle geometry characteristics required by the CONSIZ program were obtained using the solid modeling aerospace research tool (SMART).[24] The SMART is a menu-driven interactive computer program for generating three-dimensional Bezier surface representations of aerospace vehicles for use in configuration design.

Results

To perform the required mission, the propellant fraction required by the orbiter was determined by the previously described process to be 0.755 for an assumed initial T/W of 1.2. Based on this, the orbiter was determined to be 103 ft long with a wing span of 47 ft. The empty weight was estimated to be 56,300 lb and the gross weight was estimated to be 317,400 lb. To integrate this size orbiter, the booster is required to be 302 ft in length.

To investigate the effects of different combinations of airbreathing and rocket propulsion on vehicle performance and weights, rocket sea level thrust capability on the booster was varied from zero to 1,500,000 lb in increments of 250,000 lb. At each rocket thrust level, the thrust level of the airbreathing-propulsion system was varied by varying the number of engines. Rocket- and airbreathing-propulsion systems on the booster were operated in parallel for the ascent, whereas only the airbreathing system was used for cruise back. Cases where the booster was propelled by rockets alone did not include a cruise-back propellant penalty. Cruise back for an all-rocket Mach-6-staging vehicle would be impractical due to high propellant consumption. Although these cases do not have a cruise-return capability, they are included in the analysis for comparison purposes.

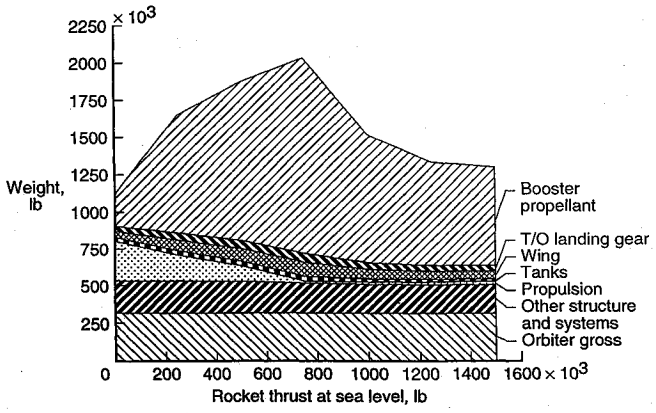

Fig. 11 Vehicle weight composition for minimum empty weight.

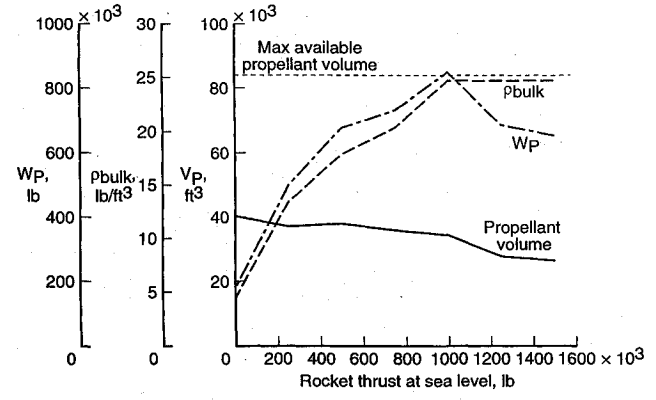

Fig. 12 Propellant characteristics for minimum gross weight.

Figure 6 shows the effect of airbreather- and rocket-thrust variations on total vehicle gross weight. Each of the constant rocket size curves has characteristics based mainly on the trade of propellant weight for propulsion system weight. As airbreather-thrust capability is increased, acceleration performance improves and propellant weight decreases. However, propulsion-system weight increases. When the weight addition due to greater numbers of airbreathing engines exceeds the reduction in propellant weight due to higher performance, the gross weight increases. A minimum weight therefore exists for each of the constant rocket-thrust curves depending on the thrust size of the airbreathing-propulsion system. Note that for the higher rocket-thrust cases, the gross weight is minimum when airbreathing engines are eliminated.

Figure 7 shows the effect of airbreather- and rocket-thrust variations on booster empty weight. The booster empty weight is greatly influenced by the size of the airbreathing system, with increasing weight for increasing airbreather thrust. This is due to the low thrust-to-weight ratio of the turboramjet propulsion system. Also shown on this figure is the minimum level of airbreathing propulsion to allow cruise back. Compared with the all-rocket-powered cases, empty weight is not significantly greater.

The minimum gross weight of each rocket-thrust curve in Fig. 6 is plotted vs rocket thrust in Fig. 8. The lowest gross weight was obtained for the all-airbreathing case. No combination of rocket and airbreathing propulsion resulted in lower gross weight. However, gross weights for the all-rocket cases begin to approach that of the all-airbreathing case with the difference being approximately 15%. It must be noted that throttling of the booster-propulsion systems was not performed in this study, but that throttling may result in lower gross weights than those obtained for the combined rocket/airbreather cases.

The minimum empty weights from the curves of Fig. 7 are plotted vs rocket thrust in Fig. 9. This figure shows that as rockets are added, airbreathing propulsion can be reduced and lower booster empty weight results. It appears from this analysis that to obtain the lowest empty weight, airbreathing propulsion should be minimized. This is true even when the booster is constrained to fly an airbreathing type constant-dynamic-pressure-path trajectory, which is not the optimum flight path for rocket-propelled vehicles.

Figures 10 and 11 show the weight composition of the vehicle for the minimum gross weight and minimum empty weight cases, respectively. These figures illustrate that variations in vehicle weight with rocket thrust are mainly due to the propellant and propulsion-system weights. Both landing gear and wing weights are a function of gross weight and both increase as gross weight increases. However, they do not impact overall weight substantially because of their low relative magnitudes. Propellant tank weight is also shown to have a small effect on vehicle weight and is relatively unchanged with changing rocket thrust.

The reason for the behavior of the propellant tank weight can be seen in Figs. 12 and 13 which show the variation in the weight, bulk density, and volume of the booster propellant as a function of rocket thrust for the minimum gross and minimum empty weight cases, respectively. Propellant tank weight is primarily a function of propellant volume. Even though the weight of the propellant increases greatly with the addition of rocket propulsion, due to the requirement for liquid oxygen, this is offset by the increase in the overall bulk density of the LH^2-LOX propellant combination. The propellant volume required remains well below that of the maximum available tank volume and even decreases for the high rocket-thrust cases.

Another effect of adding rocket propulsion is the reduction in flight times, as shown in Fig. 14. Depending on the rocket thrust, ascent times to the staging point can be reduced by 15 min or more. This may be advantageous should time to orbit become a consideration. Shorter ascent times may extend vehicle service life and may also reduce the risk of mission abort due to system failures.

Along with the decreased time to staging with rocket addition, the downrange distance to the staging point is also decreased, as shown in Fig. 15. This results in lower cruise-return propellant requirements. At high rocket-thrust levels, the downrange distance of the booster is low enough that only a minimal airbreathing capability would be required for return to the launch site.

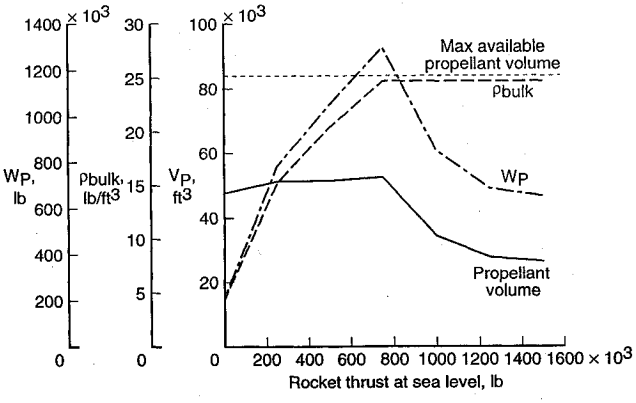

Fig. 13 Propellant characteristics for minimum gross weight.

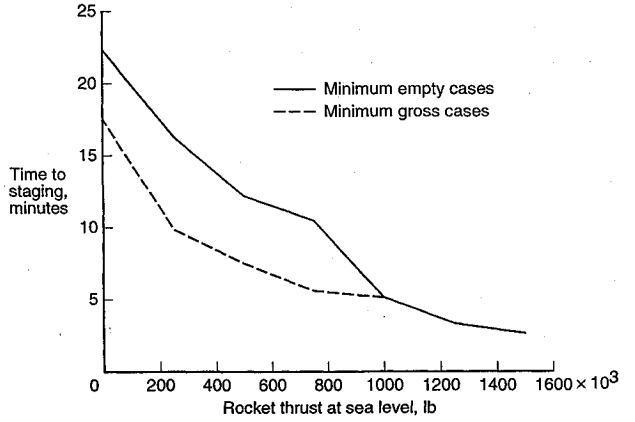

Fig. 14 Time to staging for minimum weight cases.

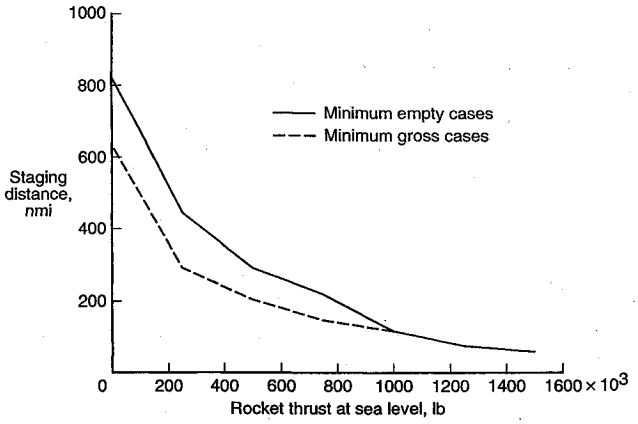

Fig. 15 Vehicle staging distance for minimum weight cases.

The airbreathing and rocket systems of the booster were not throttled during ascent to optimize performance in this study. Both rocket and airbreather engines were maintained at the highest possible thrust levels. This was done to understand the application of combined rocket and airbreathing propulsion at the most basic level. However, improvements in performance of the combined propulsion cases is likely with intermittent or throttled operation of the rocket engines as a complement to the airbreathing propulsion system. The analysis performed here should be considered as an attempt to establish a foundation upon which more detailed studies can be based.

Conclusions

A conceptual level analysis of a horizontal-takeoff two-stage-to-orbit launch vehicle consisting of an airbreathing/rocket-propelled booster and a rocket-propelled orbiter has been performed. The booster utilized turboramjet engines and linear aerospike rocket engines operating in parallel and at full thrust. The amounts of rocket and airbreathing propulsion on the booster were varied and the effects on vehicle weights and performance determined for a fixed staging velocity of Mach 6.

The lowest vehicle gross weight was obtained when the booster was propelled by all airbreathers, but this was only 15% lighter than when the booster was propelled by all rockets. None of the combined airbreathing/rocket cases resulted in lower gross weights, although only parallel operation at full thrust was investigated.

Variations in vehicle gross weight for different levels of airbreathing and rocket system thrust are mainly due to the propellant and propulsion-system weights. Landing gear, wing, and tank-weight variations have a small effect on overall weight. Propellant weight increases greatly with the addition of rocket propulsion, but the effect on propellant volume is offset by the increase in the overall bulk density of the LH_2-LOX propellant combination.

Booster empty weight is greatly influenced by the thrust size of the airbreathing system. This is due to the low thrust-to-weight ratio of the turboramjet propulsion system. As rockets are added, airbreathing propulsion can be reduced and lower booster empty weight results. The analysis indicates that to obtain the lowest empty weight, airbreathing propulsion should be minimized.

Flight time can be greatly reduced by adding rocket propulsion. Depending on the rocket thrust, ascent times can be reduced by 15 min or more in comparison with all-turboramjet-powered cases. This is a result of greater vehicle acceleration due to higher thrust-to-drag margins.

Along with the decreased time to staging with rocket addition, the downrange distance to the staging point is also decreased. This results in lower cruise-return propellant requirements. At high rocket-thrust levels, the downrange distance of the booster is small enough that only a minimal airbreathing capability would be required for return to the launch site.

Acknowledgment

The research presented in this paper is a portion of the material to be included in a Master of Science thesis with the George Washington University.

References

[1]Escher, W. J. D., and Flornes, B. J., "A Study of Composite Propulsion Systems for Advanced Launch Vehicle Applications," Marquardt Co., Marquardt Rept. 25, 194, Van Nuys, CA, Sept. 1966.

[2]Bendot, J. G., Brown, P. N., and Piercy, T. G., "Composite Engines for Application to a Single-Stage-to-Orbit Vehicle," NASA CR 2613, Dec. 1975.

[3]Martin, J. A., "An Evaluation of Composite Propulsion for Single-Stage-to-Orbit Vehicles Designed for Horizontal Take-Off," NASA TMX-3554, Nov. 1977.

[4]Martin, J. A., "Ramjet Propulsion for Single-Stage-to-Orbit Vehicles," *Journal of Spacecraft and Rockets*, Vol. 15, No. 5, 1978, pp. 259, 260.

[5]Kramer, P. A., and Bühler, R. D., "Airbreathing Booster Stages for Space Transporters Compared with Pure Rocket Systems," IAF Paper 79-09, Sept. 1979.

[6]Kramer, P. A., and Bühler, R. D., "Hybrid Rocket/Airbreathing Propulsion for Ballistic Space Transportation," *Journal of Spacecraft and Rockets*, Vol. 17, No. 4, 1980, pp. 334–341.

[7]Schoettle, U. M., "Performance Analysis of Rocket-Ramjet Propelled SSTO Vehicles," IAF Paper 85-133, Oct. 1985.

[8]Foster, R. W., Escher, W. J. D., and Robinson, J. W., "Studies of an Extensively Axisymmetric Rocket Based Combined Cycle (RBCC) Engine Powered SSTO Vehicle," AIAA Paper 89-2294, July 1989.

[9]Reed, D. A., Jr., Ikawa, H., and Sadunas, J. A., "Star-Raker—An Airbreather/Rocket-Powered, Horizontal Takeoff Tridelta Flying Wing, Single-Stage-to-Orbit Transportation System," AIAA Paper 79-0895, May 1979.

[10]Furniss, S. G., "SSTO Design Optimization," IAF Paper 89-222, Oct. 1989.

[11]Wetzel, E. D., Meadowcroft, E. T., Paris, S. W., Dunn, B. M.,Weldon, V. A., Kotker, D. J., and Williams, D. P., "Research Vehicle Configurations for Hypervelocity Vehicle Technology," Wright Research Development Center, WRDC-TR-90-3003, Vol. II, Boeing Aerospace and Electronics, Seattle, WA, April 1990.

[12]Beach, H. L., Jr., "Prospects for Future Hypersonic Air-Breathing Vehicles," AIAA Paper 91-5009, Dec. 1991.

[13]Koelle, D. E., and Kuczera, H., "Sänger Space Transportation System, Progress Report 1989," IAF Paper 89-217, Oct. 1989.

[14]Morris, R. E., and Williams, N. B., "A Study of Advanced Airbreathing Launch Vehicles with Cruise Capability," Lockheed Co., Lockheed Rept. LR 21042, Burbank, CA, Feb. 1968.

[15]Ward, B. D., Hewitt, F. A., and Mattinson, R. M., "High Speed Propulsion Assessment, Volume I—Technical Report," Air Force Wright Aeronautical Labs., AFWAL-TR-88-2005, Rolls-Royce Inc., Atlanta, GA, May 1988.

[16]Diem, H. G., and Kirby, F. M., "Linear Aerospike Engine Study, Final Report," NASA CR-135231, Nov. 1977.

[17]Divan, P. E., "Aerodynamic Analysis System for Conceptual and Preliminary Analysis from Subsonic to Hypersonic Speeds," AIAA Paper 80-1897, Aug. 1980.

[18]Braur, G. L., Cornick, D. E., and Stevenson, R., "Capabilities and Applications of the Program to Optimize Simulated Trajectories (POST)," NASA CR-2770, Feb. 1987.

[19]Seiden, E. I., Honeycutt, W. D., and Hansen, G. E., "Space Vehicle Weight Estimation Techniques," Convair Aerospace Div., General Dynamics, GDC-ERR-1527-1, San Diego, CA, Dec. 1971.

[20]Anon., "Space Shuttle Synthesis Program (SSSP), Volume II–Weight/Volume Handbook, Final Report," NASA CR-114987, Dec. 1970.

[21]Glatt, C. R., "WAATS–A Computer Program for Weights Analysis of Advanced Transportation Systems," NASA CR-2420, Sept. 1974.

[22]Anon., "Space Shuttle Mass Properties Status Report," Rockwell International Space Div., SD72-SH-0120-26, Downey, CA, Nov. 1974.

[23]Anon., "Orbiter Detail Weight Statement," Rockwell International Shuttle Orbiter Div., SD75-SH-0116-124, Downey, CA, Dec. 1985.

[24]McMillin, M. L., Rehder, J. J., Wilhite, A. W., Schwing, J. L., Spangler, J., and Mills, J.C., "A Solid Modeler for Aerospace Vehicle Preliminary Design," AIAA Paper 87-2901, Sept. 1987.

James A. Martin
Associate Editor